RESEARCH ARTICLE

AMERICAN JOURNAL OF medical genetics PART A

Clinical Delineation and Natural History of the *PIK3CA*-Related Overgrowth Spectrum**

Kim M. Keppler-Noreuil,[1]* Julie C. Sapp,[1] Marjorie J. Lindhurst,[1] Victoria E.R. Parker,[2] Cathy Blumhorst,[1] Thomas Darling,[3] Laura L. Tosi,[4] Susan M. Huson,[5] Richard W. Whitehouse,[6] Eveliina Jakkula,[7] Ian Grant,[8] Meena Balasubramanian,[9] Kate E. Chandler,[5] Jamie L. Fraser,[1] Zoran Gucev,[10] Yanick J. Crow,[5] Leslie Manace Brennan,[11] Robin Clark,[12] Elizabeth A. Sellars,[13] Loren DM Pena,[14] Vidya Krishnamurty,[15] Andrew Shuen,[16] Nancy Braverman,[17] Michael L. Cunningham,[18] V. Reid Sutton,[19] Velibor Tasic,[20] John M. Graham Jr.,[21] Joseph Geer Jr.,[22] Alex Henderson,[23] Robert K. Semple,[2] and Leslie G. Biesecker[1]

[1]National Human Genome Research Institute, National Institutes of Health, Bethesda, Maryland

[2]The University of Cambridge Metabolic Research Laboratories, Institute of Metabolic Science, Cambridge, UK

[3]Department of Dermatology, Uniformed Services University of the Health Sciences, Bethesda, Maryland

[4]Division of Orthopaedic Surgery and Sports Medicine, Children's National Medical Center, Washington, District of Columbia

[5]Manchester Centre for Genomic Medicine, Central Manchester University Hospitals NHS Foundation Trust, Institute of Human Development, Faculty of Medical and Human Sciences, University of Manchester, Manchester Academic Health Sciences Centre (MAHSC), Manchester, UK

[6]Department of Radiology, Central Manchester University Hospitals NHS Foundation Trust Manchester Royal Infirmary Oxford Road Manchester, Manchester, UK

[7]Department of Clinical Genetics, Helsinki University Central Hospital, Helsinki, Finland

[8]Department of Plastic Surgery, Cambridge University Hospitals NHS Trust, Cambridge, UK

[9]Sheffield Clinical Genetics Service, Sheffield Children's NHS Foundation Trust, Sheffield, UK

[10]Department of Endocrinology and Genetics, Medical Faculty Skopje, Skopje, Macedonia

[11]Medical Genetics, Kaiser Permanente Oakland, University of California, San Francisco, California

[12]Division of Medical Genetics, Department of Pediatrics, Loma Linda University Medical Center, Loma Linda, California

[13]Section of Genetics and Metabolism, Arkansas Children's Hospital, Little Rock, Arkansas

[14]Division of Genetics, Department of Pediatrics, Duke University Medical Center, Durham, North Carolina

[15]Pediatrics and Genetics Clinics, Alpharetta, Georgia

[16]Department of Medical Genetics, McGill University Health Centre, Montreal, Quebec, Canada

[17]Department of Human Genetics and Pediatrics, McGill University, Montreal Children's Hospital Research Institute, Montreal, Canada

[18]Division of Craniofacial Medicine, University of Washington School of Medicine, Seattle, Washington

There are no conflicts of interest declared by the co-authors; L.G.B. and M.J.L. declare receipt of royalties from Genentech, and L.G.B. declares receipt of royalties from Amgen and an honorarium from Wiley-Blackwell.

**The copyright line for this article was changed on 19 November 2014 after original online publication.

Grant sponsor: Intramural Research Program of the National Human Genome Research Institute; Grant sponsor: Wellcome Trust (Senior Research Fellowship in Clinical Science); Grant number: 098498/Z/12/Z; Grant sponsor: Clinical Research Training Fellowship; Grant number: 097721/Z/11/Z; Grant sponsor: UK National Institute for Health Research (NIHR) Cambridge Biomedical Research Centre; Grant sponsor: UK Medical Research Council Centre for Obesity and Related Metabolic Diseases.
*Correspondence to:
Kim M. Keppler-Noreuil, M.D., National Human Genome Research Institute/NIH, 49 Convent Drive 4A83, Bethesda, MD 20892.
E-mail: kim.keppler-noreuil@nih.gov
Article first published online in Wiley Online Library
(wileyonlinelibrary.com): 29 April 2014
DOI 10.1002/ajmg.a.36552

[19]Department of Molecular and Human Genetics, Baylor College of Medicine, Houston, Texas
[20]University Children's Hospital, Medical School, Skopje, Macedonia
[21]Clinical Genetics and Dysmorphology, Department of Pediatrics, Harbor-UCLA Medical Center, Los Angeles, California
[22]Greenwood Genetics Center, Greenwood, South Carolina
[23]Northern Genetics Service, Newcastle Upon Tyne Hospitals, Newcastle Upon Tyne, UK

Manuscript Received: 2 December 2013; Manuscript Accepted: 1 March 2014

Somatic mutations in the phosphatidylinositol/AKT/mTOR pathway cause segmental overgrowth disorders. Diagnostic descriptors associated with *PIK3CA* mutations include fibroadipose overgrowth (FAO), Hemihyperplasia multiple Lipomatosis (HHML), Congenital Lipomatous Overgrowth, Vascular malformations, Epidermal nevi, Scoliosis/skeletal and spinal (CLOVES) syndrome, macrodactyly, and the megalencephaly syndrome, Megalencephaly-Capillary malformation (MCAP) syndrome. We set out to refine the understanding of the clinical spectrum and natural history of these phenotypes, and now describe 35 patients with segmental overgrowth and somatic *PIK3CA* mutations. The phenotypic data show that these previously described disease entities have considerable overlap, and represent a spectrum. While this spectrum overlaps with Proteus syndrome (sporadic, mosaic, and progressive) it can be distinguished by the absence of cerebriform connective tissue nevi and a distinct natural history. Vascular malformations were found in 15/35 (43%) and epidermal nevi in 4/35 (11%) patients, lower than in Proteus syndrome. Unlike Proteus syndrome, 31/35 (89%) patients with *PIK3CA* mutations had congenital overgrowth, and in 35/35 patients this was asymmetric and disproportionate. Overgrowth was mild with little postnatal progression in most, while in others it was severe and progressive requiring multiple surgeries. Novel findings include: adipose dysregulation present in all patients, unilateral overgrowth that is predominantly left-sided, overgrowth that affects the lower extremities more than the upper extremities and progresses in a distal to proximal pattern, and in the most severely affected patients is associated with marked paucity of adipose tissue in unaffected areas. While the current data are consistent with some genotype–phenotype correlation, this cannot yet be confirmed.

Key words: somatic mosaicism; *PIK3CA* gene; fibroadipose overgrowth; segmental overgrowth; macrodactyly; CLOVES syndrome

How to Cite this Article:
Keppler-Noreuil KM, Sapp JC, Lindhurst MJ, Parker VER, Blumhorst C, Darling T, Tosi LL, Huson SM, Whitehouse RW, Jakkula E, Grant I, Balasubramanian M, Chandler KE, Fraser JL, Gucev Z, Crow YJ, Brennan LM, Clark R, Sellars EA, Pena LDM, Krishnamurty V, Shuen A, Braverman N, Cunningham ML, Sutton VR, Tasic V, Graham JM, Geer J, Henderson A, Semple RK, Biesecker LG. 2014. Clinical delineation and natural history of the *PIK3CA*-related overgrowth spectrum.

Am J Med Genet Part A 164A:1713–1733.

INTRODUCTION

Next generation sequencing has resulted in major advances in understanding the molecular etiology of somatic overgrowth syndromes [Lindhurst et al., 2011; Lindhurst et al., 2012; Kurek et al., 2012; Lee et al., 2012; Raffan and Semple, 2011; Rivière et al., 2012; Shirley et al., 2013]. Since the finding in 2011 that Proteus syndrome is caused by somatic activating mutations in the growth-promoting serine/threonine kinase AKT1, multiple subsequent reports have described activating mutations in other signaling proteins in the same RTK/PI3K/AKT/mTOR growth pathway in several different segmental overgrowth syndromes. The mutated genes include *PIK3CA*, *PIK3R2*, *AKT3* and *mTOR* [Lindhurst et al., 2012; Kurek et al., 2012; Lee et al., 2012; Poduri et al., 2012; Rivière et al., 2012; Rios et al., 2013]. Some mutations have been found in more than one phenotypically distinct disorder, and this overlap raises the important question of the relative contributions of underlying genotype, of timing of the mutation and of the precise cell of origin of the founder mutation during development to the ultimate clinical phenotype. A particularly encouraging aspect of recent genetic findings is that the pharmaceutical industry is engaged in a major effort to develop drugs targeting this pathway for use in cancer. This means that these genetic discoveries have brought the prospect of targeted drug trials in segmental overgrowth dramatically closer. Critical to the planning of effective trials will be an understanding of the natural history of the different *RTK/PI3K/AKT/MTOR*-related overgrowth disorders.

One of the recently described segmental overgrowth phenotypes caused by mutations in the *PIK3CA* gene is fibroadipose overgrowth (FAO) [Lindhurst et al., 2012]. The major manifestation of this disorder is segmental and progressive overgrowth of subcutaneous, muscular, and visceral fibroadipose tissue, sometimes associated with skeletal overgrowth. We now provide further details of eight of the patients with this disorder previously described in an abbreviated form [Lindhurst et al., 2012] (a ninth patient from that report was not included because she was the subject of a recent clinical report [Tziotzios et al., 2011]) and present 27 additional patients with a broader range of phenotypic manifestations who have not been reported. We describe their genotypes, phenotypes, and natural history to better characterize and refine their diagnoses with the aims of delineating genotype-phenotype correlations, assisting clinicians in their diagnostic efforts, and ultimately aiding the identification of target populations for the trial of candidate disease-modifying therapies.

MATERIALS AND METHODS

Patients

This study was reviewed and approved by the Institutional Review Board of the National Human Genome Research Institute (94-HG-0132) and the NRES Committee East of England—Cambridge South (12-EE-0405). The patients described herein were ascertained from a larger group of patients with overgrowth (fibroadipose and skeletal tissues) and other findings including vascular and lymphatic malformations and skin and other abnormalities. These patients were referred to the NIH (National Institutes of Health) or to the University of Cambridge for inclusion in research studies for evaluation of overgrowth. Medical records, including photographs, were reviewed initially. All participants had physical examinations by the coauthors and other studies, including X-rays or other imaging of affected areas. Thirteen of 35 patients were also evaluated in person at the NIH.

Study Procedures

Candidate lesions for biopsy were selected based on clinical assessment that the tissue was overgrown, had a vascular malformation, or an epidermal nevus. Most samples were derived from standard punch biopsies although a few were derived from deeper tissues collected during surgery performed for clinical indications, typically aimed at mitigating the functional or cosmetic consequences of overgrowth. The cells were grown from tissue explants in DMEM. Molecular analysis consisted of candidate mutation analysis for somatic mutations in *PIK3CA* using a custom PCR restriction assay as described in Lindhurst et al. [2012] for the p.His1047 mutations. For p.Glu542Lys, DNA was amplified using the following primers: (6FAM)-TCTGTAAATCATCTGTGAATCCAGAGGG and 5′-CTTTCTCCTGCTCAGTGATTC followed by digestion with XbaI. For p.Glu545Lys, DNA was amplified using the following primers: 5′-CTACACGAGATCCTCTCTCTGAAATCATT and (6FAM)- TGCTGAGATCAGCCAAATTCAG followed by digestion with MseI. For p.Cys420Arg, DNA was amplified using the following primers: (6FAM)-CCCATTATTATAGAGATGATTGTTG and 5′-ACAAGTTTATATTTCCCCATGCCAATGGCC followed by digestion with MspI. Most samples were tested in duplicate and mutation levels were averaged. If multiple cultures were established from the same piece of tissue or if multiple direct DNA extractions were done from the same specimen, the range of mutation level is reported. Mutation analyses were performed on blood samples in 21/35 patients and on saliva in 3/35 (Patients 4, 18, 21).

CLINICAL REPORTS

(Available as supplementary online material at http://wileyonlinelibrary.com/journal/ajmg)

RESULTS

The molecular diagnoses in these 35 patients were determined by the presence of a somatic *PIK3CA* mutation, found in the affected tissues at varying levels, and not in the blood or saliva, as described in each clinical summary and in Table I. We reviewed the clinical and radiological findings in each patient focusing on features described in Lindhurst et al. [2012] and features associated with Proteus syndrome, which is summarized in Table II. The ordering of patients in the table was informally ranked from mild to severe. All patients had overgrowth consistent with what we have previously described as fibroadipose tissue. The assessment of severity was subjective; unilateral was considered milder than bilateral in most cases, a greater number of findings was considered more severe than fewer findings, and more surgeries performed in the past was considered more severe. We did not construct a formal global severity score as this was challenging considering the range of the effects in the patients. Most of the severely affected patients were previously designated as having CLOVES syndrome [Sapp et al., 2007] and had most or all of the characteristic features of CLOVES syndrome.

The most common mutation was the p.His1047Arg (H1047R) occurring in 19/35 (54%) patients. The distribution of the other mutations was: p.His1047Leu (H1047L) in 8/35 (23%) patients, p. Glu545Lys (E545K) in 4/35 (11%) patients, p.Glu542Lys (E542K) in 3/35 (8%) patients, and p.Cys420Arg (C420R) in 1/35 (3%) patients.

There was a qualitative correlation of these genotypes with the overall phenotypes. Twenty-five of 35 (71%) patients had a phenotype most consistent with the either FAO, Hemihyperplasia-Multiple Lipomatosis (HHML) or macrodactyly phenotypes, and all but two of these patients had either p.His1047Arg or p. His1047Leu. The other mutations that were found in this group were *PIK3CA* p.Glu542Lys, and p.Glu545Lys. In those 9/35 (26%) individuals with the CLOVES syndrome phenotype the distribution of mutations was as follows: three with p.His1047Arg, three with p.Glu545Lys, two with p.Glu542Lys, and one with p. Cys420Arg (Fig. 1).

Thirty-one of 35 patients had congenital manifestations, except for one identified between the ages of 2 and 3 months, two between 12 and 18 months, and one at puberty. Four patients had findings that were detectable prenatally. The age range at our evaluation was 1–49 years with the mean age 14.5 years, and the median 7 years. Five patients were greater than 40 years old. The male to female ratio was 1:1.3 (15 males to 20 females, binomial $P \approx 0.5$).

All 35 individuals had asymmetric, disproportionate overgrowth, which was sporadic, and had a progressive course. This overgrowth was predominantly in the limbs or fingers/toes (Fig. 2 A–G). More individuals had involvement of the lower extremities (24/35) than upper extremities (6/35, $P = 0.041$), and three of 35 had overgrowth of both upper and lower extremities. The remaining two of 35 patients had overgrowth involving the midline (back, trunk) and no extremities. The extent of involvement of the extremities in descending order of frequency, was: combinations of toes, feet, leg (N = 14) > toes and feet (N = 6) > toes only (N = 3) > fingers and hands (N = 2) or hand and arm (N = 2) or toes/feet/leg and fingers (N = 2) > legs only (N = 1). Two of the patients with the combination of toes, feet and legs affected also had

TABLE I. Mutation Levels in Tissues and Cultured Cells

Patient	Anatomical source[a]	Tissue mutation level (%)[b]	Cultured cells mutation level (%)[c]
1 H1047R	Fatty tissue—left toe	13	—
2 H1047R	Bone—left second toe	—	28
	Skin—left second toe	—	17–28
3 H1047R	Skin—right third finger	50	—
	Bone—right third finger	8	—
4 H1047L	Neural—right third finger	5	—
	Blood	0	—
	Saliva	0	—
5 H1047L	Skin—left 2nd toe	5	—
	Blood	0	—
6 (N68) H1047R	Skin—left second finger ulnar surface	—	<1–5
	Blood	0	—
7 H1047R	Subcutis—left second toe	—	17
	Bone—left second toe	—	10–23
8 (N110) H1047R	Skin—medial tip of second left toe	7	31
	Blood	0	—
9 E542K	Skin piece 1—left foot	—	29
	Skin piece 2—left foot	—	24–28
10 (N104) H1047R	Skin—left hand	—	2
	Blood	0	—
11 H1047R	Skin—right great toe	3	6
	Skin—right ankle	2	2
	Skin—left thigh	0	0
	Skin—upper left arm	0	0
12 H1047L	Skin—left foot	—	24
	Fatty tissue—left foot	—	24
	Blood	0	—
13 H1047L	Skin—left toe	—	25
	Blood	0	—
14 (N109) H1047R	Skin—dorsal left foot	12–26	24–37
	Blood	0	—
15 E545K	Skin—right foot	9	—
	Blood	0	—
16 H1047R	Fibrofatty tissue—right side of abdomen	1	—
17 (N99) H1047R	Growth plate—left second toe proximal phalanx	31	—
	Growth plate—left second toe middle phalanx	22	—
	Growth plate—left second toe distal phalanx	25	—
	Growth plate—left third toe proximal phalanx	27	—
	Growth plate—left third toe middle phalanx	9	—
	Growth plate—left third toe distal phalanx	14	—
	Skin—webbing between second and third toes	—	33
	Bone—left talus	—	3–6
	Bone—phalanx, right second toe	—	4–10
	Nerve—left foot	—	9
	Vessel 1—left foot	—	25
	Vessel 2—left foot	—	14

TABLE I. (*Continued*)

Patient	Anatomical source[a]	Tissue mutation level (%)[b]	Cultured cells mutation level (%)[c]
	Blood	0	—
18 H1047L	Fibrofatty tissue—right foot	39	—
	Saliva	0	—
19 H1047R	Nerve—left anterior tibial nerve	7	—
	Nerve—left posterior tibial nerve	7	26
	Adipose tissue piece 1—posterior left leg	9	29–33
	Adipose tissue piece 2—posterior left leg	10	27–33
	Connective tissue—posterior left leg	—	4
	Muscle—posterior left leg	3	0–1
	Tendon—posterior left leg	0	0
	Skin—posterior left leg	4	8–22
20 H1047R	Skin—left forearm	—	2
	Skin—right forearm	—	0
	Lipoma—left forearm	25	—
	Blood	0	—
21 (M001) H1047L	Adipose tissue—left leg	39	—
	Muscle—left leg	33	—
	Fibrous tissue—left leg	32	—
	Skin—left leg	24	50
	Bone—left leg	8	—
	Skin—left arm	—	0
	Blood	0	—
	Saliva	0	—
22 (N7) H1047R	Articular cartilage—left foot	—	33
	Adipose tissue—left foot	—	33
	Bone—left foot	—	33
	Skin—left foot	—	33
	Muscle—left foot	—	16
	Deep tissue—left foot	—	7
	Blood	0	—
23 (N108) H1047L	Skin—left leg	3	—
	Adipose tissue—left leg	4	—
	Blood	0	—
24 E545K	Lymphatic malformation—back	<1—1	—
	Skin over lymphatic malformation—back	0	—
	Blood	0	—
25 E545K	Skin—right foot, second metatarsal	7	12–15
	Growth plate—right foot, second metatarsal	11	15–17
26 H1047R	Skin, left buttock	—	4
	Skin, right upper inner arm	—	0
27 (N45) H1047R	Skin—ankle	—	<1–2
	Blood	0	—
28 E545K	Fat and fascia—left proximal tibia	0	0
	Fat and fascia—left distal femur	1	3
	Soft tissue—foot	6	—
	Growth plate—toe	—	11
	Normal skin—left tibia	0	0
29 E542K	Lymphatic malformation—left trunk	—	5
	Skin—left leg	—	<1
30 H1047R	Skin—abdomen	7	0
	Tonsil—left	0	0
	Tonsil—right	0	0
	Blood	0	—

(*Continued*)

TABLE I. (Continued)

Patient	Anatomical source[a]	Tissue mutation level (%)[b]	Cultured cells mutation level (%)[c]
31	LVEN—right side of neck; keratinocytes	—	26
E542K	LVEN—right side of neck; fibroblasts	—	0
	Skin—right side of neck; keratinocytes	—	0
	Skin—right side of neck; fibroblasts	—	0
	Blood	0	—
32	Skin—back ; keratinocytes	—	47
C420R	Skin—back; fibroblasts	—	39–52
	Skin—left dorsal foot	12	48
	Blood	0	—
33	Skin—left post. thoracic spine	25	—
H1047R	Blood	0	—
34	Angiokeratoma—trunk	5	9
H1047R	Lipoma—trunk	22	22
	Skin over lipoma—trunk	6	30
	Normal skin and fat—trunk	3	13
	Blood	0	—
35	Spinal tissue—1st Neurofibroma	7	—
H1047L	Spinal tissue—2nd Neurofiboma	3	—
	Dermis—posterior thoracic region	0	—

[a]Description of the source tissue for mutation analyses.
[b]Percentage of mutant allele as determined by the appropriate custom PCR restriction assay in DNA extracted dircetly from tissue. Range indicates mutation levels if multiple extractions were done from the same specimen.
[c]Percentage of mutant allele as determined by the appropriate custom PCR restriction assay in DNA extracted from cultured cells. Range indicates mutation levels if multiple cultures were established from the same specimen.

unilateral involvement of the orbit and cheek, and one had asymmetric overgrowth of the chest and torso. Two patients had involvement of the chest and torso, but not the limbs. The distal portion of the limbs was often the first to show observable overgrowth and subsequent progression more proximally. For example, multiple patients who initially presented with only macrodactyly of the toes had progression to the foot followed by involvement of the leg. The proximal portions of the limbs were almost never affected alone without involvement of distal structures. There was only one patient identified with only an affected leg and none with only an affected arm.

Twenty-one of 35 (60%) had unilateral overgrowth, with 15/21 (71%) being affected on the left side (binomial $P = 0.078$). Twelve of 35 had bilateral involvement in which seven of the 12 had the left side more affected than the right (binomial $P = 0.774$). Overall, the left was affected more than the right in 22/33 patients ($P = 0.081$). The tissues involved in the overgrowth were fibrous, lipomatous, vascular, and skeletal. Information regarding infiltration of lipomatous tissue into the muscle was available on 21 patients and occurred in 12/21 (57%) of these patients. Adipocellular investment into internal structures was identified in nine patients and involved the viscera (liver, spleen, pancreas), intestines, mediastinum, and spine (Fig. 3A–C).

Regional reduction of adipose tissue occurred in of 10 of 33 patients (30%) and involved the upper extremities and/or torso (chest/upper abdomen) in all these individuals, one of whom also had reduced adipose tissue of the leg unaffected by overgrowth (Fig. 3A1, A2 and B2, B4). Patient 22 had increase in subcutaneous fat in the areas where he previously had reduced adipose tissue after resection of areas of adipose overgrowth; he also maintained normal weight to height ratio despite having the multiple large masses.

None of the patients we report met the diagnostic criteria for Proteus syndrome [Biesecker, 2006], although all the patients met the general criteria, and some exhibited components of the three specific diagnostic criteria categories. Specifically, none had cerebriform connective tissue nevi (CCTN). A linear epidermal nevus was present in 4/35 patients (Fig. 4A and B), while an ovarian cyst was documented in two patients, and one individual had an unilateral ovarian cystadenoma. Dysregulated adipose tissue (either lipomatous lesions or regional lipohypoplasia) was seen in all patients, and there were 15/35 patients (43%) with vascular malformations, including capillary venous or lymphatic malformations. Some of these 15 individuals had combined venous/lymphatic malformations. However, there were no individuals with lung bullae, nor the Proteus syndrome facial phenotype.

Other limb findings included postaxial or preaxial polydactyly and cutaneous syndactyly, which involved only the toes. In particular, four had polydactyly: two with postaxial polydactyly (one unilateral left foot and one bilateral feet), one central and one with preaxial polydactyly (of the hallux). There were seven with cutaneous syndactyly: two with unilateral 2–3 toes, two with unilateral 2–4 toes, one bilateral with 2–5 toes (Right) and 2–4 toes (Left), and two unspecified (Fig. 5A–C).

Kidney abnormalities were reported in 11/26 (42%) of patients evaluated. These abnormalities included nephrogenic rests, pelviectasis, dilated ureters, hydronephrosis, duplicated renal arteries, renal cysts, and enlarged kidney(s). One patient thought to have Wilms tumor by imaging instead had benign renal lesions (nephrogenic rests on pathological examination).

TABLE II. Summary of Clinical Findings

Patient designation	1 (M013)	2 (N136)	3 (M023)	4 (M016)	5 (M026)	6 (N68)	7 (N143)	8 (N110)	9 (N144)	10 (N104)	11 (N124)	12 (N128)
Mutation	p.H1047R	p.H1047R	p.H1047R	p.H1047L	p.H1047L	p.H1047R	p.H1047R	p.H1047R	p.E542K	p.H1047R	p.H1047R	p.H1047L
Original summary phenotype	Macrodactyly	HHML	Macrodactyly	Macrodactyly	Macrodactyly	FAO	FAO	HHML	FAO	HHML	FAO	HHML
Age at time of evaluation	8 y	13 d	2y	45 y	5 y	49 y	18 m	3 y	11 m	12 y 6 m	32 y	7 y
Age at onset of symptoms	Birth	Birth	Birth	Birth	Birth	Birth	Prenatal	2–3 m	Birth	Birth	1.5 y	Prenatal
Sex	F	F	F	M	F	M	F	M	M	F	F	F
Sporadic	Y	Y	Y	Y	Y	Y	Y	Y	Y	Y	Y	Y
Mosaic	Y	Y	Y	Y	Y	Y	Y	Y	Y	Y	Y	y
Epidermal nevus	N	N	N	N	N	N	N	N	N	N	N	N
Ovarian cystadenoma(s)	N	N	N	N	N	N	N	N	N	N	N	N
Testicular/ epididymal abnormalities	N	N	N	N	N	N	N	N	N	N	N	N
Asymmetric, disproportionate overgrowth	Y	Y	Y	Y	Y	Y	Y	Y	Y	Y	Y	Y
Fibroadipose overgrowth	Y	Y	Y	Y	Y	Y	Y	Y	Y	Y	Y	Y
Affected areas of overgrowth (initial)	Lt great toe	Lt 2 toe	Rt 3, 4 fingers	Rt 3, 4 fingers	Lt 1, 2 toes	Lt 2, 3 fingers	Lt 2 toe	Lt 1, 2 toes	Lt 1–3 toes, foot	Lt thumb	Rt 1 toe, foot	Lt 1, 2 toes
Lipomatous infiltration of muscles	N	N	N	NA	N	NA	N	NA	N	NA	NA	NA
Lipomatous infiltration of internal structures	N	N	N	NA	N	NA	N	N	N	NA	PVNS	N

(Continued)

TABLE II. (Continued)

Patient designation	1 (M013)	2 (N136)	3 (M023)	4 (M016)	5 (M026)	6 (N68)	7 (N143)	8 (N110)	9 (N144)	10 (N104)	11 (N124)	12 (N128)
Regional lipohypoplasia (affected areas)	N	N	N	N	N	N	N	N	N	N	N	N
Vascular malformations (one or more)	N	N	N	N	N	Y	N	N	N	N	N	N
Polydactyly	N	N	N	N	N	N	N	N	N	N	N	N
Syndactyly	N	N	N	N	N	N	N	N	N	N	N	N
Kidney abnormalities	N	N	N	NA	N	NA	N	N	N	NA	N	Y (Lt kidney enlg'd)
Other malformations	Rt ear microtia	N	N	Y (ganglion cyst)	N	N	Y (Rt preaur pit)	N	N	N	N	N
Other skin abnormalities	N	N	N	Y (CAL)	N	N	N	Y-dermal melano-cystosis	N	N	N	N
Natural history features												
General growth (Wt/HT, centile)	NA	44/80	25/9–25	>95/50	9–25/2–9	95/25	97/90	25/25	65–70/50	90/90	NA	25 birth
OFC (centile)	50	29	25	>95	.4	>97	75	90	25	60	NA	NA
Development	NA	nl	nl	NA	NA	NA	nl	NA	nl	nl	NA	NA
Progression of fibroadipose dysregulation	Y: prog Lt 1 toe	Y: incr 1 toe	Y: prog Rt 3, 5 fingers	Y: prog incr 3,4 fingers	Y: prog Lt 1, 2 toes	Y: enlg'd fingers to Lt palm	Y: to Lt 1 toe & foot	Y: to Lt foot	Y: to Rt peri-umbilical & Lt foot	Y: to Lt thenar emin & 2 finger	Y: to Rt leg	Y: to Lt 3 toe, foot & leg
Surgeries (remove overgrown tissue/ amputations)	Y (1/0)	Y (1/0)	Y (0/2)	Y (2/0)	N	Y (2/1)	Y (1/1)	N	N	Y (1/0)	Yes, multiple	N
Scoliosis	N	N	N	N	N	N	N	N	N	N	N	N

TABLE II. (*Continued*)

Patient designation	13 (N145)	14 (N109)	15 (M027)	16 (M017)	17 (N99)	18 (M011)	19 (N116)	20 (N119)	21 (M001)	22 (N7)	23 (N108)	24 (N167)
Mutation	p.H1047L	p.H1047R	p.E545K	p.H1047R	p.H1047R	p.H1047L	p.H1047R	p.H1047R	p.H1047L	p.H1047R	p.H1047L	p.E545K
Original summary phenotype	HHML	FAO	FAO	FAO	FAO	FAO	FAO	FAO	FAO	FAO	FAO	CLOVES
Age at time of evaluation	4.5 y	5 y	2y	32 y	20 m	9 y	5 y	49 y	27 y	17 y	7 y	NB
Age at onset of symptoms	Birth	Birth	Birth	Birth	Prenatal	Birth	Birth	Birth	Birth	BIRTH	Birth	Birth
Sex	F	F	F	M	F	M	M	F	F	M	F	M
Sporadic	Y	Y	Y	Y	Y	Y	Y	Y	Y	Y	Y	Y
Mosaic	Y	Y	Y	Y	Y	Y	Y	Y	Y	Y	Y	Y
Epidermal nevus	N	N	N	N	N	N	N	N	N	N	N	N
Ovarian Cystadenoma(s)	N	N	N	N	N	N	N	N	Ovarian cyst	N	N	N
Testicular/ epididymal abnorm	N	N	N	N	N	N	N	N	N	Y (hydrocele)	N	NA
Asymmetric, disproportionate overgrowth	Y	Y	Y	Y	Y	Y	Y	Y	Y	Y	Y	Y
Fibroadipose overgrowth	Y	Y	Y	Y	Y	Y	Y	Y	Y	Y	Y	Y
Affected areas of overgrowth (initial)	Lt foot, 2–4 toes	Lt 1 & foot	Bilat feet	Rt leg, abd; Lt foot	Bilat: Lt 1–3, Rt 1, 2 toes; Lt > Rt leg	Rt leg	Lt 2–5 toes, foot, leg	Lt hand, 1, 2 fingers	Bilat feet & legs	Lt leg, buttock, foot	Rt foot, leg	Rt arm, hand
Lipomatous infiltration of muscles	Y	NA	NA	NA	NA	Y	N	Y (biceps, nerves)	NA	Y (Lt glut, paraspinal)	Y (intrafascial RLQ, Lt thigh)	NA
Lipomatous infiltration of internal structures	N	N	NA	NA	NA	Y	N	N	NA	T11-L4, pancreas	Lt intra-abdominal	Y

(*Continued*)

TABLE II. (*Continued*)

Patient designation	13 (N145)	14 (N109)	15 (M027)	16 (M017)	17 (N99)	18 (M011)	19 (N116)	20 (N119)	21 (M001)	22 (N7)	23 (N108)	24 (N167)
Regional lipohypoplasia (affected areas)	N	N	N	N	N	Y	N	N	Y (upper body)	Y (upper body)	Y (upper torso, arms, face)	N
Vascular malformations	N	N	N	N	N	N	Y (prom. vasc Lt calf)	Y (legs, feet)	N	N	Y (prom vasc)	Y (Rt thorax, neck, axilla)
Polydactyly	N	N	N	N	N	N	Y (Lt foot PA)	N	N	Y (Lt foot C)	N	N
Syndactyly	Y (2–4 toes)	Y (2–3 toes)	N	Y	Y (2–3 toes)	Y	N	N	Y (2–4 toes)	N	N	N
Kidney abnormalities	N	N	Y (enlg'd Rt, cysts)	N	NA	N	Y (Lt pelviec)	NA	NA	NA	Y (bilat NR)	NA
Other malformations	N	N	Y	N	N	N	N	N	N	Y (DM 1)	N	CHDs
Other skin abnormalities	NA	N	Y (hypopig)	N	N	N	Y (PN, CM, hypopig)	N	N	N	Y (PN)	N
Natural history features												
General growth (Wt/Ht CENTILE)	NA	25/50	50/75	>95/50	NA	60/50	80/75–90	90–95/50	>95/50	50/50–75	70/37	90/95
OFC (centile)	NA	10	~25	NA	NA	50	75%	30–40	NA	NA	91	>95
Development	nl	NA	NA	NA	NA	NA	NA	NA	NA		NA	NA
Progression of fibroadipose dysregulation	Y: to Lt leg (femoro-glut region); recurrence of Lt foot	Y: to Lt foot; Lt leg (prog involvement buttock.lab maj)	Y: prog Bilat feet	Y: prog Rt leg, abd	Y: to Lt 4 toe, Bilat forefeet; Lt chest, abd, groin	Y: prog Rt leg, buttock	Y: incr Lt leg, foot	Y: to Lt arm, shoulder	Y: prog of legs, Rt abd	Y: prog of leg, glut, vertebrae	Y: prog Rt foot, leg	Y:prog of Rt arm, hand
Surgeries (remove overgrown tissue/ amputations)	Y (1/1)	Y (2/1)	N	Y (1/0)	Y (2/0)	Y (6/2)	Y (4/2)	Y (6/3)	Y (3/1)	Y (~9/1)	Y (>3/0)	Y (1/0)
Scoliosis	N	N	N	Y	N	N	N	N	Y	N	N	N

TABLE II. (Continued)

Patient designation	25 (N147)	26 (N138)	27 (N45)	28 (N22)	29 (N164)	30 (N123)	31 (N113)	32 (N146)	33 (M028)	34 (N170)	35 (M021)
Mutation	p.E545K	p.H1047R	p.H1047R	p.E545K	p.E542K	p.H1047R	p.E542K	p.C420R	p.H1047R	p.H1047R	p.H1047L
Original summary phenotype	CLOVES	FAO	FAO	CLOVES	CLOVES	CLOVES	CLOVES	CLOVES	CLOVES	CLOVES	ENS
Age at time of evaluation	7 y	14.5 y	31 y	16 y	8 m	4 y	43 y	46 y	2 y	8 m	21 y
Age at onset of symptoms	Birth	Birth	Birth	Birth	Prenatal	~1 y	Birth	Birth	Birth	Birth	Puberty
Sex	F	F	M	M	M	F	F	F	M	M	M
Sporadic	Y	Y	Y	Y	Y	Y	Y	Y	Y	Y	Y
Mosaic	Y	Y	Y	Y	Y	Y	Y	Y	Y	Y	Y
Epidermal nevus	N	N	N	N	N	N	Y	Y	Y	N	Y
Ovarian cystadenoma(s)	N	N	N	N	N	N	Ovarian cyst	Y (unilateral)	N	N	N
Testicular/epididymal abnormalities	N	N	Y (hydrocele)	Y (hydrocele)	Bilat hydrocele	N	N	N	N	NA	NA
Asymmetric, disproportionate overgrowth	Y	Y	Y	Y	Y	Y	Y	Y	Y	Y	Y
Fibroadipose overgrowth	Y	Y	Y	N	Y	Y	Y	Y	Y	Y	N
Affected areas of overgrowth (initial)	Bilat toes (Rt 1–5 Lt 2–4), feet	Bilat feet: Lt > Rt; Lt leg	Bilat legs, Lt > Rt legs, feet, toes, abd	Bilat 1–3 toes; Lt chest	Bilat axillae, Lt scrotum, leg. Rt chest	Bilat feet, legs Lt > Rt; enlg' d fem; lipom spine, back, abd, chest	Rt foot, thigh, hand; tongue masses	Lt HH; Lt 4, 5 toes	Lt HH, Lt HM, Lt hemifacial	Back, abd	Multiple spinal tumors
Lipomatous infiltration of muscles	N	Y (muscles of legs, feet)	Y (bilat legs, Rt buttock)	Y	Y	Y	Y (Lt foot, T1-4 paraspinal)	Y (RLQ; Rt chest, Lt shoulder)	NA	N	N
Lipomatous infiltration of internal structures	Y	Y	Y (incr'd visc fat; bowel wall)	NA	Y	Y (intestinal and spinal	Y (liver, spleen, mediastinal)	Y	Y	N	N
Regional lipohypoplasia (affected areas)	N	Y (rest of body, Rt leg)	Y (UEs; torso)	N	NA	Y (chest and arms)	Y (Chest)	N	Y	Y (buttocks)	N
Vascular malformations (one or more)	Y	Y (prom veins of legs, abd, upper back)	Y (bowel)	Y (testes, cutan Lt chest)	Y	Y (bilat prom leg veins)	Y (Rt abd, back, groin; mult hemang)	Y (Lt chest, abd, pelvis; mult LA of spinal cord, muscles, liver, spleen)	N	Y	Y (large central artery in lipoma in post thoracic region)

(Continued)

TABLE II. (Continued)

Patient designation	25 (N147)	26 (N138)	27 (N45)	28 (N22)	29 (N164)	30 (N123)	31 (N113)	32 (N146)	33 (M028)	34 (N170)	35 (M021)
Polydactyly	N	Y (Bilat PA feet)	Y (L dupl hallux)	N	N	N	N	N	N	N	Y
Syndactyly	N	N	Y (2–5 toes Rt; 2–4 toes Lt)	N	N	N	N	N	N	N	N
Kidney abnormalities	N	Y (VUR, HN, enlg'd Bilat)	Y (dilated coll system)	Y (Rt > Lt enlg'd)	Y (HN)	N	Y (cysts)	N	N	Y (Bilat pelviec)	Y (duplic renal arts)
Other malformations	N	Y (fused metatarsals, Rt hip sublux, elong vert)	Y (congen hip dislocation)	N	N	Y (cerebral infarcts; vert abnorms	Y	Y (spina bifida occulta; bowel malrot; uterine fibroid)	N	Y (tethered cord)	Y (Ectasia of aorta)
Other skin abnormalities	Y	Y (hyper-pig with hair decr'd hair Lt leg)	Y: hypopig	NA	N	Y: hyperpig scalp; CM legs, Lt foot	Y (CAL cutaneous blebs)	Y	N	N	Y (mult EN; large lipoma on back)
Natural history features											
Growth (Wt/HT centile)	50/25	50/<5	10–25/25–50	50/75	90/30	50/<3	>97/<3	NA	NA	>95/>95	NA
OFC	50	<3	~75	97	15	<3	75–95>97	NA	NA	55	>95
Development	nl	NA	NA	Y/ADHD	Gross motor delay	nl	NA	nl	NA	Delayed	NA
Progression of fibroadipose dysregulation	Y: prog macrodactyly and enlarged feet	Y: prog Lt leg, foot; incr'd fatty infiltration in abd)	Y: prog legs, feet, subcutan, intra-abd wall, viscera, bowel; irregular fem	Y: to Rt 3, 4 fingers, chest/back, Bilat legs, feet (Lt > Rt)	Y	Y: prog legs, feet; masses in chest, back, abd, spine	Y: prog legs, feet; masses in chest, back, abd, spinal r	Y: prog buttocks, feet, toes, leg (Lt > Rt)	Y: prog Lt leg, buttock, face, ear, tongue, gingiva	Y	N
Surgeries (remove overgrown tissue/ amputations)	Y (3/2)	N	Y (18/1)	Y (3–5/2)	Y (1/0)	Y (3/1)	Y (8–9/0)	Y (>10/0)	Y (2/0)	Y (1/0)	Y (4/0)
Scoliosis	Y	Y	N	N	N	Y	Y	Y	N	N	Y

<, less than; >, greater than; abnorms, abnormalities; ADHD, attention deficit hyperactivity disorder; aff, affected; arts, arteries; Bilat, Bilateral; CAL, café-au-lait macule; CLOVES, congenital lipomatosis, overgrowth, vascular malformations, and epidermal nevi, scoliosis/skeletal/spinal; coll, collecting; congen, congenital; CHDs, congenital heart defects; cutan, cutaneous; CM, cutis marmorata; decr'd, decreased; DM 1, type 1 diabetes mellitus; duplic, duplicated; elong, elongated; emin, eminence; enlg'd, enlarged; ENS, epidermal nevus syndrome; FAO, fibroadipose overgrowth; fem, femoral head; F, female; glut, gluteus/gluteal; hemang, hemangiomas; HH, hemihyperplasia; HM, hemimegalencephaly; HHML, hemihyperplasia multiple lipomatosis; HN, hydronephrosis; Ht, Height; hyperpig, hyperpigmented macule; hypopig, hypopigmented macules; incr, increase; lab maj, labia majora; Lt, Left; lipom, lipomatous; LA, lymphangiomatous; M, male; malrot, malrotation; mult, multiple; m, month; NA, not available; NB, newborn; NR, nephrogenic rests; nl, normal; N, no; OFC, occipito-frontal circumference; pelviec, pelviectasis; PN, pigmented nevus; PVNS, pigmented villonodular synovitis of right knee; PA, postaxial; preaur, preauricular; prom, prominent; prog, progressive; Rt, right; RLQ, right lower quadrant of abdomen; subcutan, subcutaneous; sublux, subluxation; vasc, vasculature; vert, vertebral; VUR, vesicoureteral reflux; Wt, weight; y, year; Y, yes. Note that the centiles are approximate in many cases. Original Summary Phenotype is our diagnosis, prior to the recognition, from analyzing these data that all seem to be a single continuous phenotypic spectrum.

Key: Shading: original 8 cases Lindhurst et al. [2012].

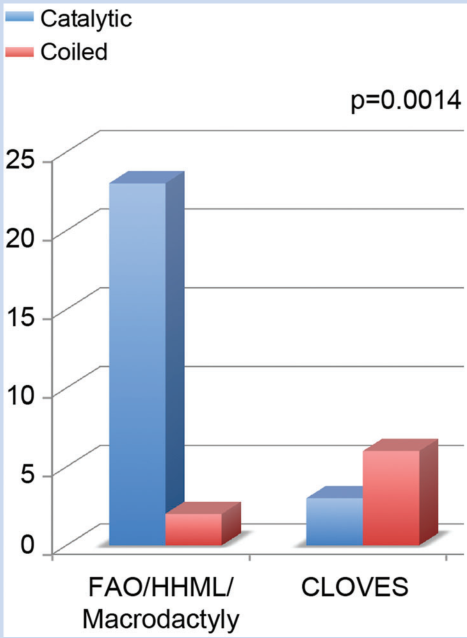

FIG. 1. Genotype/Phenotype Correlations in 35 patients with the predicted amino acid changes from *PIK3CA* mutations. When the predicted mutations are categorized by the two main functional domains of the protein (coiled vs. catalytic domains), there is a correlation of the domain location and phenotype ($P = 0.0014$).

Other skin abnormalities included a dermal melanocytic nevus, café-au-lait macules, hypopigmented macules, cutis marmorata, pigmented nevi, and patchy hyperpigmentation in 12/33 (36%) patients. Other malformations (minor and major) found in these patients (13/34 or 38%) included one patient with two cerebral infarcts (one was neonatal in onset), one with hemimegalencephaly, one with congenital heart defects (multiple VSDs, ASD), inguinal hernias, bowel malrotation, hip subluxation/dislocation, spina bifida occulta, tethered cord, extra segments in the vertebrae, uterine fibroids, and splenic cysts, and the remainder with minor anomalies including one with ganglion cyst and one with right preauricular pit. One patient had type 1 diabetes mellitus. Spinal and major nerve neurofibromas were also reported in two patients. Patient 35 had biopsy-proven spinal neurofibromas removed at several levels; *NF1*, *NF2*, and *PTEN* genes had been tested and were normal. These patients did not have other manifestations of Neurofibromatosis, types 1 or 2. In Patient 21, her lumbosacral plexus had multiple nodular lesions on MRI that have been asymptomatic.

Growth patterns (weight and height) were generally normal with weight and heights between the 25th and 95th centiles, with the exception of three patients with heights <5th centile. Head circumferences showed macrocephaly or relative macrocephaly in eight of 27 (30%) patients.

Developmental milestones and cognitive abilities were apparently normal in almost all individuals, except for two who had developmental delays on their evaluations at 8 months in two patients, and one who had delay at 2 years. The latter patient had hemimegalencephaly. The patient with two cerebral infarcts found in the neonatal period had normal cognitive testing at 4 years of age. One patient was reported to have ADHD, but primary test data were not available.

Patient 21 had a history of thrombosis in a spinal vertebral artery, but no associated abnormality of vasculature. There have been no identified malignancies in these patients.

Twenty-nine individuals had surgeries to manage overgrowth. Fifteen had amputations of the affected leg or digits. In multiple patients, there was continued growth in the affected limb after surgical amputation.

DISCUSSION

The recent finding of *PIK3CA* mutations in a spectrum of overlapping forms of overgrowth affords the opportunity to gain insight into the pathophysiologic basis of these conditions, and suggests that a reappraisal of current clinical classification is timely. This study provides a clinical and molecular evaluation of 35 patients with *PIK3CA* somatic mutations.

Novel Findings

Novel overgrowth findings in these patients included: adipose dysregulation present in all patients, unilateral overgrowth that was predominantly left-sided, overgrowth that affected the lower extremities more than the upper extremities and progressed in a distal to proximal pattern, and in the most severely affected patients was associated with marked paucity of adipose tissue in unaffected areas. While not statistically significant, when overgrowth was asymmetric, it was often left-sided. Larger patient numbers are needed to assess whether this is significant. The underlying mechanism for the observed distal to proximal pattern of progression of overgrowth with only one patient showing earlier proximal involvement is unknown at present. There also was statistically significant association of genotypes with phenotypic groupings within the spectrum of *PIK3CA* somatic mutations. All but two of the patients with the phenotype most consistent with either FAO, HHML, or macrodactyly designations had a mutation in the catalytic domain (codon1047), while the majority of patients with the CLOVES syndrome designation had mutations in the coiled domain with a *P* value of 0.0014 (Fig. 1).

Clinical Classification

The previously reported phenotypic descriptors in patients with *PIK3CA* somatic mutations included FAO [Lindhurst et al., 2012], HHML [Biesecker et al., 1998] and CLOVES syndrome [Sapp et al., 2007; Alomari, 2009; Kurek et al., 2012], isolated macrodactyly [Rios et al., 2013], and the megalencephaly syndrome, MCAP [Rivière et al., 2012]. The present study focused on patients with non-CNS phenotypes. Patients previously diagnosed with FAO, HHML, CLOVES syndrome, and isolated macrodactyly [Lindhurst et al., 2012; Kurek et al., 2012; Lee et al., 2012; Rios et al., 2013] had considerable overlap and we were unable to discern a rational boundary that would separate FAO, HHML, or macrodactyly. In all three, there was congenital, static, or mildly progressive asymmetric

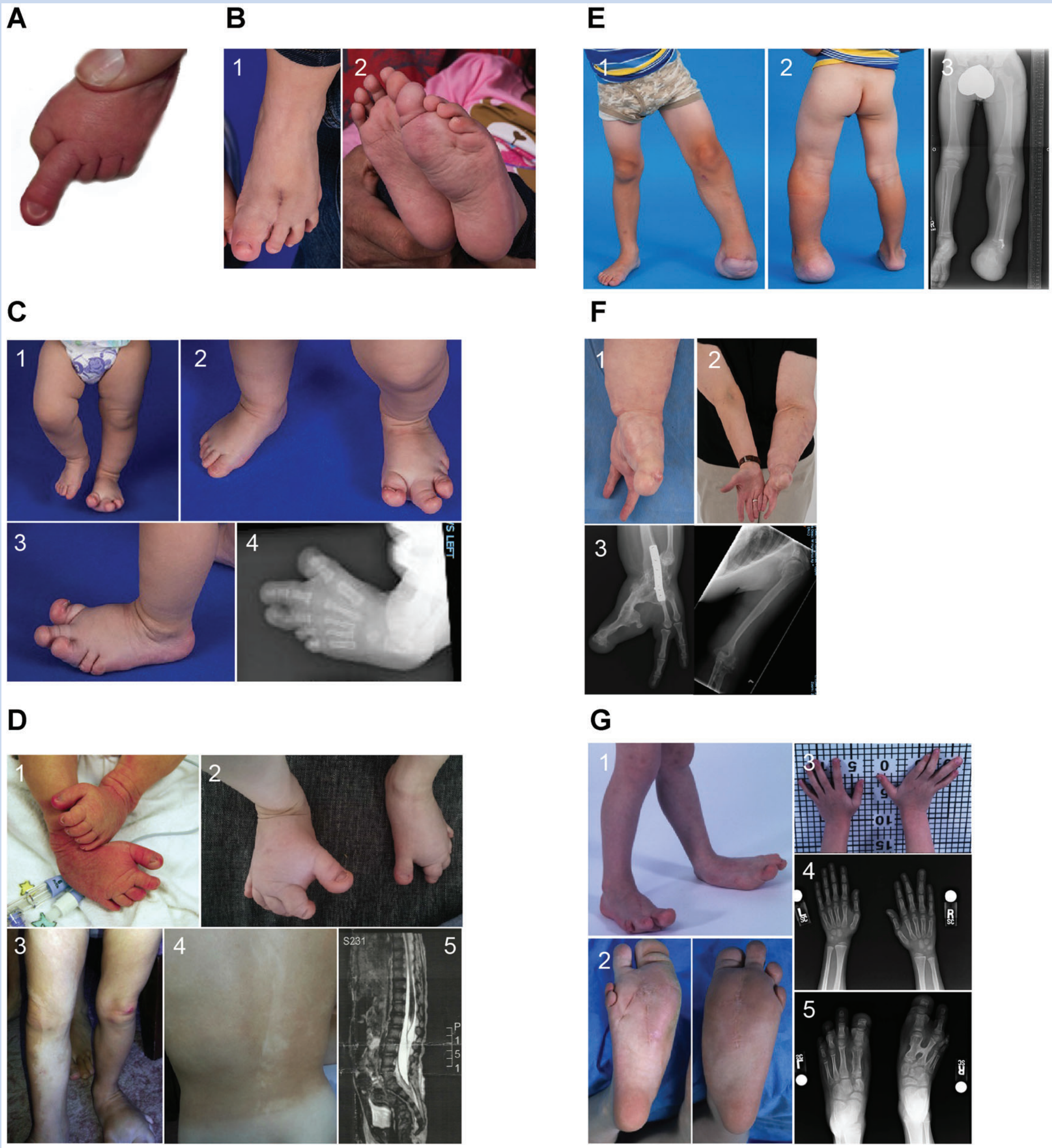

FIG. 2. Spectrum of overgrowth in patients with somatic *PIK3CA* mutations (A) Patient 2 at 13 days of age with macrodactyly of the left second toe; (B) Patient 7 at 18 months of age (1) Dorsal view of the left foot with overgrowth following surgical resection of T2, (2) Ventral views of both feet show overgrowth of the middle to distal ventral region of the left foot; (C) Patient 9 at 11 months of age (1–3) Enlargement of the left T1—3 with ballooning appearance of the distal portion, and increased circumference and length of the entire left foot, (4) X-ray of the left foot shows enlarged phalanges of T1–3; (D) Patient 15 (1) At 1 day of age, an enlarged right foot, (2) At 18 months of age, medial deviation and progressive widening of both feet, (3) Areas of hypopigmentation on the legs and (4) back, (5) T1-weighted MRI scan shows a cystic lesion adjacent to the lumbar spine; (E) Patient 19 at 5 years 6 months of age (1) Frontal view shows overgrowth of the left leg following trans-tibial amputation at four years of age, (2) Posterior view of the legs, (3) X-ray of the legs shows an enlarged left femur, tibia and fibula; (F) Patient 20 at 49 years of age (1) Enlarged left shoulder, arm and hand: left F4, 5 appeared normal, left F2,3 are missing following surgical amputation, and there is a 2 cm lipoma between the PIP and DIP joints of F4, (2) Left F1 is enlarged and surgically repositioned, (3) X-rays show her hand following surgical resection of F2, 3 and an enlarged left humerus; (G) Patient 28 at 10 years of age (1 and 2) Enlargement of the feet and legs, more severe on the left, (3) Enlargement and angular deformity of the right F3, 4, (4) X-rays of the hands show bone and soft tissue overgrowth of the phalanges of the right F3, 4, (5) X-rays of the feet: left foot shows four toes following surgical resection of T2, 3 and overgrowth of the metatarsals, the right foot shows four toes with absent T2, overgrowth of metatarsals and phalanges of T1 and T3, bony fusion with an "H" configuration of metatarsals of T1 and T3, and small second cuneiform.

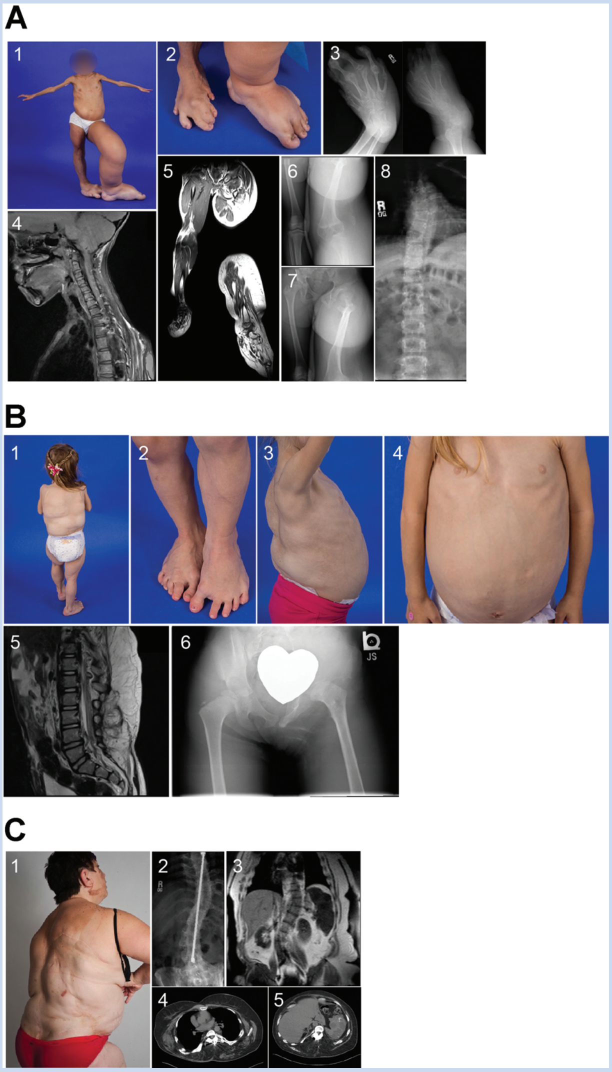

FIG. 3. Spectrum of overgrowth in patients with somatic *PIK3CA* mutations. A: Patient 26 at 14 years 6 months of age (1) Frontal view shows the upper body lipohypoplasia and bilateral leg overgrowth, more severe on the left, (2) Dorsal view of the feet show bilateral postaxial polydactyly with more severe overgrowth of the left foot, (3) X-rays of the feet: the right foot shows marked overgrowth of the metatarsals of T1—4, unusual epiphyses of all rays, and a supernumerary metatarsal, the left foot shows six toes with an enlarged metatarsal of T1 and proximal fusion of the metatarsal bones, (4) MRI of the lateral spine shows a large mass over her upper thoracic region; multiple neural foraminal masses at several levels in the thoracic spine, some of these are associated with dural ectatic changes and prominent CSF in the nerve root sheath, (5) MRI scan of the legs shows extensive soft tissue overgrowth, primarily in the fatty tissues with fat tissue intermixed with muscle in the left leg, (6 and 7) X-rays of the pelvis and legs show marked asymmetry and enlargement of the left hemipelvis and leg, completely dislocated left hip with unusual overgrowth pattern of the lesser trochanter and proximal femur, an enlarged left distal femur, particularly the medial femoral condyle, a displaced left patella, an abnormal configuration of the left anterior tibia, and an enlargement and bowing of the left fibula, subluxation with shallow acetabulum of the right hip, and overgrown and elongated right fibula and greater trochanter, (8) X-rays of the spine show scoliosis of the mid-thoracic spine centered at T6, and elongated and overgrown lower thoracic and lumbar vertebral bodies; (B) Patient 30 at 4 years of age (1) Posterior view of her whole body shows multiple lipomatous lesions involving her abdomen, chest and back, and upper body lipohypoplasia, (2) Views of her legs and feet show asymmetry of the leg positioning and size, widened feet with splayed toes with the left side larger than the right, and the left leg with prominent superficial veins, (3) Lateral view shows her barrel-chest and prominent abdomen with multiple lipomatous masses involving her abdomen and back, (4) Frontal view shows her chest and arms with lipohypoplasia, and protuberant abdomen with multiple lipomatous masses, (5) MRI scan of the lateral lower thoracic, lumbar and sacral vertebrae shows multi-level foraminal soft tissue masses, some of which are associated with dural ectatic changes, and subcutaneous soft tissue masses most compatible with the lipomas involving the back, and the extra segmentation in coccyx, (6) X-ray of the pelvis and upper legs shows right hip dislocation, abnormal acetabulum and femoral head; (C) Patient 31 at 43 years of age (1) Posterior view of her head, back and abdomen shows multiple masses and scars on her back from surgical excision of the venolymphatic malformations, and an epidermal nevus on her right cheek and pinna, (2) X-ray of the spine shows thoraco-lumbar scoliosis following surgical rod placement, (3–5) MRI scans of the chest, abdomen, and pelvis show scoliosis, marked fatty intermixture of the paraspinal muscles, splenomegaly with multiple cysts, irregular enhancement of the muscles of the posterior chest wall on the left, obesity with marked intra-abdominal fat, periaortic and paracaval foci compatible with additional collateral vessels or small vascular masses, and grossly normal caliber of the superior and inferior vena cava, the thoracic and abdominal aorta, and the common iliac vessels.

overgrowth associated with areas of increased subcutaneous adipose tissue. This study included four patients who had only macrodactyly, although this macrodactyly was also associated with overgrowth of adipose tissue.

The CLOVES syndrome manifests prenatal asymmetric overgrowth that is primarily proportionate in nature [Sapp et al., 2007; Alomari, 2009]. Affected persons commonly had splayed feet and toes. The vascular malformations were most commonly combined lymphatico-venous anomalies with cutaneous blebbing and weeping. The lipomatous nature of the overgrowth was characterized by overgrowth of fat within normal fatty fascial planes and linear verrucous epidermal nevi. CLOVES syndrome has also been associated with CNS abnormalities [Sapp et al., 2007; Alomari, 2009]; there was only one patient with hemimegalencephaly confirmed in this series. The patients described here were previously designated as having CLOVES syndrome if they had congenital lipomatous overgrowth, vascular malformations, and skeletal/spinal involvement with or without the presence of the epidermal nevi. Three of nine patients with the phenotype of CLOVES syndrome had epidermal nevi. One of the four patients in this study with clinical findings of Epidermal Nevus Syndrome had epidermal nevi. On

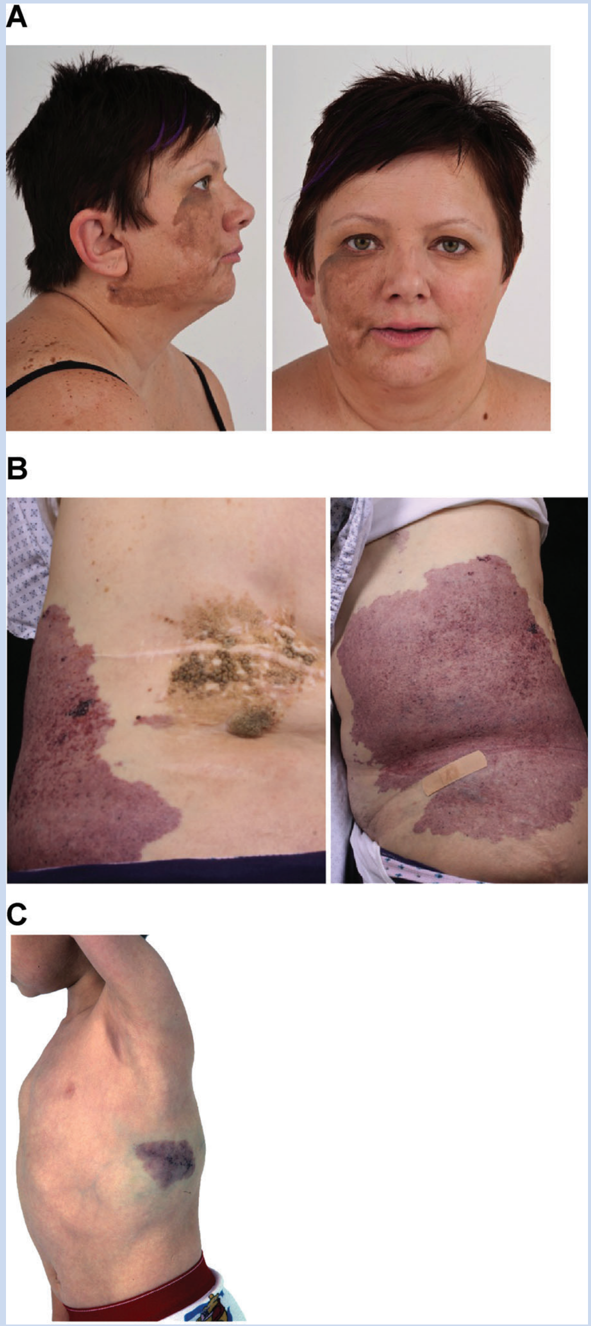

FIG. 4. Epidermal nevi and vascular malformations in patients with somatic *PIK3CA* mutations. A: Patient 31 at 43 years of age shows an epidermal nevus involving the right cheek, pinna and neck, (B) Patient 32 at 46 years of age shows an epidermal nevus and vascular malformation involving the abdomen, (C) Patient 28 at 10 years of age shows a vascular malformation involving the left trunk

reviewing all of the patients here, we conclude that it may be difficult to distinguish those patients described as having CLOVES syndrome from more severe FAO/HHML if they have an epidermal nevus or vascular malformations.

We conclude that the phenotypic descriptors of FAO, HHML, and macrodactyly associated with *PIK3CA* mutations are not sufficiently distinct to warrant separate clinical descriptors. Further, the descriptor of CLOVES syndrome may reside at an extreme of the spectrum formerly including FAO, HHML, and macrodactyly.

Many of these patients had previous diagnoses including Klippel–Trenaunay syndrome (KTS) and Proteus syndrome, however, they did not meet published diagnostic criteria for either condition. Once again, however, there was overlap of findings in these patients with those disorders. Klippel–Trenaunay syndrome manifests both overgrowth and vascular malformations. However, in KTS the

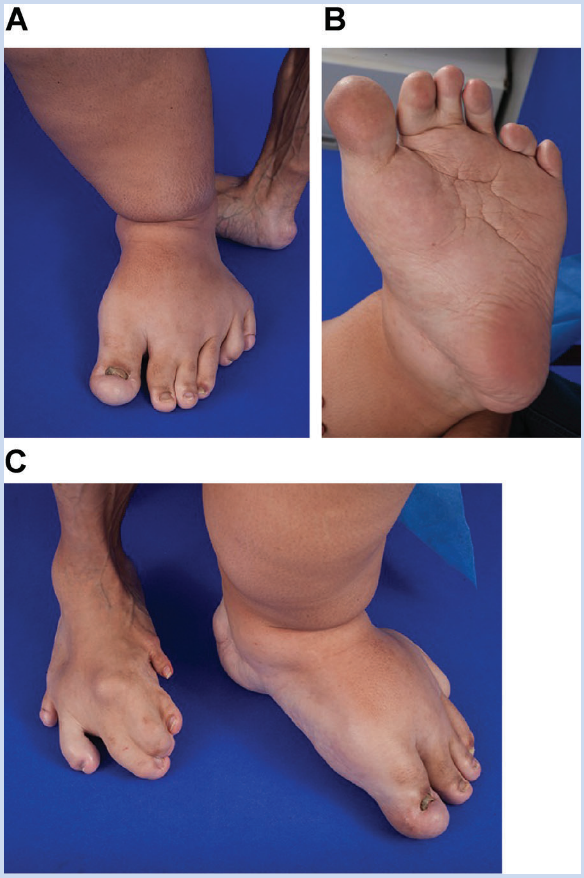

FIG. 5. Polydactyly and cutaneous syndactyly. Patient 26 at 14 years 6 months of age (A) Dorsal view of the left foot and (B) Ventral view of the left foot show both show widening and postaxial polydactyly with shortened T5, 6 and partial cutaneous syndactyly of T2, 3, and wrinkling of the skin of the sole of the foot, (C) Dorsal view of the feet and ankles shows bilateral postaxial polydactyly, overgrowth of the left foot and leg, and the right foot with decreased subcutaneous tissue, prominent veins, and abnormal toes including small T1, 6, complete cutaneous syndactyly of T3, 4, and overgrowth of T3, 4, 5.

overgrowth is generally ipsilateral and overlapping with the vascular malformations. The typical vascular malformation is the lateral venous anomaly, and the skeletal overgrowth lacks the distortion and progressivity seen in persons with Proteus syndrome [Biesecker et al., 1998; Cohen, 2000], and the patients reported here. Moreover, the patients currently described lack the hallmark skin finding of Proteus syndrome (CCTN), as noted in Table II.

Genotype–Phenotype Correlation

Our data suggest that some genotype–phenotype correlation may exist, that is, there are recognizable patterns of overgrowth associated with the five different mutations identified in these 35 patients. The most frequently identified *PIK3CA* mutation was in codon 1047 (27 patients), and the predominant feature in patients with that mutation was a progressive, mosaic phenotype of FAO with other areas of deficient adiposity in those with severe overgrowth, but less frequently associated with vascular malformations. Of the 27 patients with codon 1047 mutations, 19 had p.His1047Arg substitution and eight had p.His1047Leu substitution. Of these 27 patients, 14 were previously diagnosed by us as having FAO, five were diagnosed with HHML, four were diagnosed with macrodactyly, three were diagnosed with CLOVES syndrome, and one with possible Epidermal Nevus Syndrome.

Those having a phenotype more compatible with CLOVES syndrome had a mix of less frequently observed mutations, including p.Glu542Lys, p.Glu545Lys, and p.Cys420Arg, as well as p. His1047Arg, similar to the six patients reported by Kurek et al. [2012]. Genetic studies of further patients with CLOVES syndrome may provide a better understanding of the distribution of causative somatic mutations within *PIK3CA*.

The mutations within *PIK3CA* were detected in affected tissues or cultured cells at varying levels, but not detected in the blood (in 21 patients) or saliva (in three patients). There was not a clear correlation of mutation level in either tissues or cultured cells to either the quality (nature) of the manifestations or the overall severity of the manifestations. Patient 1, who was considered to be mildly affected, had a mutation burden of 31% in the sampled affected tissue, whereas in Patient 21 the mutation burden was only 7% in the sampled tissue. We hypothesize that the overall lack of correlation of severity to mutation burden emanates from the severe sampling limitations. Our ability to sample tissues is limited both by human subjects considerations and practicality. Indeed, we predict that in the more mildly affected patients, the many unaffected areas of their bodies would show a low or zero level of the mutation, which would contrast with patients who had extensive areas of overgrowth. In contrast to our results showing an association of keratinocyte versus fibroblast mutation level with the nature of the cutaneous manifestations of Proteus syndrome [Lindhurst et al., 2014], the present study only assayed fibroblasts from biopsies.

Increased and Decreased Adipose Tissue

Some patients had striking lipoatrophy in areas not affected by overgrowth, which occurred in those who had more severe overgrowth. Further, this finding was more common in patients with CLOVES syndrome (4/9, 44%) or more severe manifestations of FAO/HHML (6/21, 28%). Interestingly, in one patient (Patient 22), when the overgrown adipose tissue was resected, there was increased deposition of fat in the areas with previously decreased adipose tissue. These observations raise questions about the role of PI3K signaling in regulation of body fat deposition. Lindhurst et al. [2012] suggested that the adipose tissue paucity in the non-overgrown areas of the patients is caused by chronic negative energy balance of adipose depots consequent to the demands of the pathologically growing and energy-sequestering adipose tissue in affected regions.

PI3K signaling activates the serine/threonine kinases AKT1, AKT2, and AKT3. AKT1 is most widely expressed, and is associated with growth [Chen et al., 2001], consistent with the Proteus phenotype, while AKT2 is highly expressed in insulin-responsive tissues including skeletal muscle, liver, and fat, and is more closely implicated in the metabolic actions of insulin [Whiteman et al., 2002]. AKT3 is most highly expressed in brain and heart, with lower expression in the tissues affected in the current patients. Somatic occurrence of both AKT2 and AKT3 p.Glu17Lys mutants, paralogous to the Proteus-associated AKT1 mutation, have been described. The AKT2 mutation causes severe insulin-independent hypoglycemia, mild asymmetric overgrowth, and progressive obesity [Hussain et al., 2011], while the AKT3 mutation was associated with brain overgrowth [Poduri et al., 2012; Rivere et al., 2012]. There was no evidence of either insulin resistance or hypoglycemia, except in one patient who had infiltration of the pancreas with fibroadipose tissue. The type 1 diabetes in this patient was attributed to the typical autoimmune pathophysiology based upon testing, and not from the pancreatic involvement with FAO.

Other Characteristic Associated Findings

Polydactyly and/or cutaneous syndactyly was seen in nine patients and exclusively involved the toes with variable pattern of involvement. The pattern of cutaneous syndactyly involved toes 2–3 and 2–4 most commonly. The frequency and pattern of polydactyly and cutaneous syndactyly in these patients suggests this is a manifestation of this spectrum of disorders. The mechanism for this finding is not known. However, this finding points to an early defect in limb patterning and involvement of the PI3K/AKT signaling pathway. One hypothesis is that the *PI3K* gene interacts with other genes involved in limb patterning, including *GLI3*. Interaction of *PI3K* and *AKT1* with *GLI3* has been demonstrated in a novel KRAS-initiated pathway leading to VMP1 in cancer cells [Lo Re et al., 2012]. Alternatively, we speculate that the overgrowth of the feet in these patients may interact with normal patterning signals and gradients, but produce polydactyly due to the increased size of the limb. In support of this hypothesis, studies by Bouldin and Harfe [2009] using the Dorking chicken mutant found that over-proliferation due to FGF signaling caused polydactyly. In addition Lu et al. [2005] found that over-expression of *Fgf4* resulted in polysyndactyly in the mouse. As FGF signaling is not a primary determinant of anterior–posterior patterning and is instead a determinant of AER size and limb growth, we suggest that activation of the AKT/PIK3CA pathway analogously increases AER and/or limb bud size.

Macrocephaly (OFC $\geq$ 90th centile) was present in 30% of patients in this study. There was only one patient with a central nervous system abnormality, hemimegalencephaly, but this is likely attributable to our ascertainment bias.

Urinary and kidney abnormalities were found in approximately 40% of the patients; however renal function was normal. Renal underdevelopment or agenesis has been reported in CLOVES syndrome, but not in those with FAO or macrodactyly [Alomari, 2009; Kurek et al., 2012; Lindhurst et al., 2012].

Natural History

Onset of overgrowth in the majority of patients was congenital and documented prenatally in four. Often, there was infiltration of the fibroadipose tissue into muscle and visceral organs often causing secondary enlargement; therefore, the overgrowth primarily was in fibroadipose tissue rather than from enlargement of the actual muscle or visceral tissue. The nature of the overgrown tissue was best exemplified by patient 19, where serial sections of an amputated leg show that this limb was almost entirely fibroadipose tissue, but also demonstrated radiolographically in patients 17 and 26. Furthermore, the overgrowth was progressive in all patients, in size and sometimes also in location with spread involving adjacent areas. However, bilateral involvement did not correlate with the age of the patient at evaluation, suggesting that bilateral manifestations are not simply due to age.

Treatment of segmental overgrowth disorders has relied upon surgical debulking [Biesecker, 2006] and orthopedic procedures to limit growth [Tosi et al., 2011]. The majority (83%) of these 35 patients had surgical interventions for their overgrowth, many with multiple surgeries including 43% with amputations of affected limbs and or digits. These interventions occurred throughout the patients' early childhood and into adulthood. It is clear from the patients presented herein that there is marked variability in rate of progression and number of complications. More longitudinal clinical data are needed regarding natural history on the effects of rate of overgrowth at different ages and after surgical debulking.

Potential Tumorigenesis and Cancer Risk and Surveillance Recommendations

While there were no identified malignancies in these patients, two patients had tumors, one with potential premalignant findings of nephrogenic rests, and another with ovarian cystadenoma, which has not been reported previously. In addition, Kurek et al. [2012] reported one patient with p.His1047Arg mutation having Wilms tumor. The catalytic subunit of phosphatidylinositol-3-kinase (PI3K) is somatically mutated in many cancers including colorectal, ovarian, breast, and hepatocellular carcinomas, and in glioblastomas [Vivanco and Sawyers, 2002; Campbell et al., 2004; Lee et al., 2005; Levine et al., 2005; Li et al., 2005; Velho et al., 2005; Yuan and Cantley, 2008]. These *PIK3CA* mutations were located mostly at hotspots within the helical domain (encoded by exon 20), and they resulted in gain of function mutations that were implicated in oncogenicity [Samuels et al., 2004; Ikenoue et al., 2005; Kang et al., 2005]. Recently, Cizkova et al. [2013] found that patients with HER2-positive breast cancer, having *PIK3CA* mutation positive tumors, which were treated with trastuzumab, had a worse outcome than those with wild-type tumors. Given the prevalence of *PIK3CA* codon H1047 mutations in cancer, a critical consideration is whether patients with these mutations are at increased risk of malignancy. Transgenic expression of the *Pik3ca* p.His1047Arg mutation in lung [Engelman et al., 2008], or breast epithelium [Adams et al., 2011; Meyer et al., 2011] in mice has been shown to produce malignant tumors. However, in these studies mutant *Pik3ca* was overexpressed, potentially exaggerating its oncogenicity. Expression of *Pik3ca* p.His1047Arg at endogenous levels in mouse ovaries did not produce tumors after 1 year [Kinross et al., 2012]. It is possible that expression at endogenous levels in the cellular context of human mesodermal lineages has more benign consequences than implied by the mouse models overexpressing mutant *Pik3ca*. It is of note that codon 1047 oncogenic *PIK3CA* mutations are common in benign seborrheic keratoses and epidermal nevi in humans [Hafner et al., 2007], demonstrating that there is no obligate association of these mutations to malignancy. However, longitudinal studies are needed to properly assess this potential risk and to formulate surveillance recommendations, should such a risk be identified.

Current recommendations for tumor surveillance are based upon a reported Wilms tumor in a patient with CLOVES syndrome [Kurek et al., 2012] and of nephrogenic rests (a premalignant tumor) in one of the patients reported here. Although the evidence is not sufficient to demonstrate high risk, it may be prudent to consider serial abdominal ultrasounds every 3–4 months until age 8 years in all patients with a somatic *PIK3CA* mutation similar to the recommendations in isolated hemihyperplasia and Beckwith–Wiedemann syndrome. In addition, because of the finding of spinal root and major nerve neurofibromas, as well as lipomatous lesions involving the spine, neurological monitoring, and spinal MRI scan should be considered in patients with truncal involvement. Finally, a reported risk of pulmonary embolism in patients with CLOVES syndrome having thoracic and central phlebectasia [Alomari et al., 2010] and as presented in this series, spinal thrombosis in patient 21 and neonatal cerebral infarcts in patient 30 suggest that it is important to be aware of the possible associated thrombosis risk in this group of patients. It is known that the related disorder, Proteus syndrome also has an increased risk of thrombosis, and consideration of anticoagulant prophylaxis is recommended in patients undergoing surgery or other procedures that may predispose to deep venous thrombosis or pulmonary embolism.

These patients should be monitored for other potential associated complications, including vascular malformations and skeletal and spinal abnormalities. More specific recommendations for surveillance will be forthcoming based upon analyses in a larger population of patients with *PIK3CA* somatic mutations.

Implications for Design of Future Therapeutic Trials

The results of this study highlight the need to collect specific clinical data prospectively to design future clinical trials. Clinical information regarding the assessment of cosmetic and functional parameters affected by the overgrowth, including but not limited to mobility, extent of vascular malformations and its associated risks, ventilation and metabolic status is essential in these patients to understand natural history fully, as well as to evaluate treatment effectiveness. Future targeted therapies may be possible with the identification of activated PI3K/AKT signaling, either through inhibition of PI3K, of AKT, or of downstream pathways such as mTORC1, using clinically available drugs. Rapamycin was reportedly beneficial in a child with type II segmental Cowden syndrome associated with PTEN deficiency [Marsh et al., 2008]. Patients with colorectal cancer and tumor positive for *PIK3CA* mutations, who are treated with aspirin may have prolonged survival [Ogina et al., 2013; Printz, 2013; Sahin and Garrett, 2013; Viudez et al., 2013]. Intensive efforts are underway to develop novel inhibitors for use in cancer. The progressive nature of this disorder makes it a good target for pharmaceutical therapy because downregulation of the pathway may prevent the disease progression that is seen in many of the patients reported here.

In conclusion, based upon the results of this clinical and molecular analysis of 35 patients, we propose that the clinical entities formerly described as FAO, HHML, macrodactyly, and CLOVES syndrome caused by *PIK3CA* somatic mutations represent a single phenotypic spectrum. CLOVES syndrome represents a more severe subset of that spectrum. In addition, previous authors [Lee et al., 2012; Mirzaa et al., 2012; Rivière et al., 2012] have described the megalencephaly syndromes that have overlapping findings with CLOVES, FAO and HHML. Therefore, we propose the phenotypic designation of *PIK3CA*-Related Overgrowth Spectrum. While Mirzaa et al. [2013b] proposed a similar designation, “PIK3CA-related segmental overgrowth”, our designation is distinct for the following reasons: (1) the absence of the term “segmental” because there are patients having the *PIK3CA* somatic mutation who present with bilateral and systemic involvement, and (2) the inclusion of the term, “spectrum” to emphasize that there are different but related phenotypes rather than one specific phentoype. There is evidence of a correlation of genotype and phenotype, with CLOVES syndrome associated with coiled domain mutations and the FAO/HHML/macrodactyly phenotype associated with mutations in the catalytic domain. The overgrowth findings most commonly involve the lower extremities. Our data also suggest that the distal limb is affected more often than is the proximal segment, and with progression involves more proximal structures. Other characteristic associated findings include polydactyly (all types) and cutaneous syndactyly (together or separately), kidney and urinary tract abnormalities, and occasionally, abnormalities of the ovaries (cysts) and testes (hydroceles). Longitudinal studies of larger cohorts are needed to determine the rate and extent of bony and muscular involvement, as well as the pathogenetic mechanisms causing the distinct manifestations associated with somatic *PIK3CA* mutations. We recommend testing for the *PIK3CA* mutations on affected tissues in a patient presenting with any of the key features described herein.

ACKNOWLEDGMENTS

The authors are especially grateful to the patients and their families who participated in this research study. We also thank, Professor John Fallon of the University of Wisconsin for his insights into the mechanisms of polysyndactyly, Hadley Bloomhardt for laboratory support, and the staff, surgeons, and providers who were instrumental in obtaining clinical information and the specimens used for analysis including Drs. Dale J. Townsend, Angus Dobbie, Molly Crenshaw, and Alexandra Baumgarten. This research was supported by the Intramural Research Program of the National Human Genome Research Institute. R.K.S. and V.E.R.P. are supported by the Wellcome Trust (Senior Research Fellowship in Clinical Science 098498/Z/12/Z and Clinical Research Training Fellowship 097721/Z/11/Z, respectively), by the UK National Institute for Health Research (NIHR) Cambridge Biomedical Research Centre, and by the UK Medical Research Council Centre for Obesity and Related Metabolic Diseases.

REFERENCES

Adams JR, Xu K, Liu JC, Agamez NM, Loch AJ, Wong RG, Wang W, Wright KL, Lane TF, Zacksenhaus E, Egan SE. 2011. Cooperation between Pik3ca and p53 mutations in mouse mammary tumor formation. Cancer Res 71:2706–2717.

Alomari AI. 2009. Characterization of a distinct syndrome that associates complex truncal overgrowth, vascular, and acral anomalies: A descriptive study of 18 cases of CLOVES syndrome. Clin Dysmorphol 18:1–7.

Alomari AI, Alomari AI, Burrows PE, Lee EY, Hedequist DJ, Mulliken JB, Fishman SJ. 2010. CLOVES syndrome with thoracic and central phlebectasia: Increased risk of pulmonary embolism. J Thorac Cardiovasc Surg 140:459–466.

Biesecker LG, Peters KF, Darling TN, Choyke P, Hill S, Schimke N, Cunningham M, Meltzer P, Cohen MM Jr. 1998. Clinical differentiation between Proteus syndrome and hemihyperplasia: Description of a distinct form of hemihyperplasia. Am J Med Genet 79:311–319.

Biesecker LG. 2006. The challenges of Proteus syndrome: Diagnosis and management. Eur J Hum Genet 14:1151–1157.

Bouldin CM, Harfe BD. 2009. Aberrant FGF signaling, independent of ectopic hedgehog signaling, initiates preaxial polydactyly in Dorking chickens. Dev Biol 334:133–141.

Campbell IG, Russell SE, Choong DY, Montgomery KG, Ciavarella ML, Hooi CS, Cristiano BE, Pearson RB, Phillips WA. 2004. Mutation in *PIK3CA* gene in ovarian and breast cancer. Cancer Res 64:7678–7681.

Chen WS, Xu PZ, Gottlob K, Chen ML, Sokol K, Shiyanova T, Roninson I, Weng W, Suzuki R, Tobe K, Kadowaki T, Hay N. 2001. Growth retardation and increased apoptosis in mice with homozygous disruption of the Akt1 gene. Genes Dev 15:2203–2208.

Cizkova M, Dujaric ME, Lehmann-Che J, Scott V, Tembo O, Asselain B, Pierga JY, Marty M, de Cremoux P, Spyratos F, Bieche I. 2013. Outcome impact of *PIK3CA* mutations in HER2-positive breast cancer patients treated with trastuzumab. Br J Cancer 108:1807–1809.

Cohen MM Jr. 2000. Klippel-Trenaunay syndrome. Am J Med Genet 93: 171–175.

Engelman JA, Chen L, Tan X, Crosby K, Guimaraes AR, Upadhyay R, Maira M, McNamara K, Perera SA, Song Y, Chirieac LR, Kaur R, Lightbown A, Simendinger J, Li T, Padera RF, García-Echeverría C, Weissleder R, Mahmood U, Cantley LC, Wong KK. 2008. Effective use of PI3K and MEK inhibitors to treat mutant Kras G12D and *PIK3CA* H1047R murine lung cancers. Nat Med 14:1351–1356.

Hafner C, López-Knowles E, Luis NM, Toll A, Baselga E, Fernández-Casado A, Hernández S, Ribé A, Mentzel T, Stoehr R, Hofstaedter F, Landthaler M, Vogt T, Pujol RM, Hartmann A, Real FX. 2007. Oncogenic *PIK3CA* mutations occur in epidermal nevi and seborrheic keratosis with a characteristic mutation pattern. Proc Natl Acad Sci USA 104:13450–13454.

Hussain K, Rocha N, Payne F, Minic M, Thompson A, Daly A, Scott C, Harris J, Smillie BJ, Savage DB, Ramaswami U, De Lonlay P, O'Rahilly S, Barroso I, Semple RK. 2011. An activating mutation of AKT2 and human hypoglycemia. Science 334:474.

Ikenoue T, Kanai F, Hikiba Y, Obata T, Tanaka Y, Imamura J, Ohta M, Jazag A, Guleng B, Tateishi K, Asaoka Y, Matsumura M, Kawabe T, Omata M. 2005. Functional analysis of *PIK3CA* gene mutations in human colorectal cancer. Cancer Res 65:4562–4567.

Kang S, Bader AG, Vogt PK. 2005. Phosphatidylinositol 3-kinase mutations identified in human cancer are oncogenic. Proc Natl Acad Sci USA 102:802–807.

Kinross KM, Montgomery KG, Kleinschmidt M, Waring P, Ivetac I, Tikoo A, Saad M, Hare L, Roh V, Mantamadiotis T, Sheppard KE, Ryland GL, Campbell IG, Gorringe KL, Christensen JG, Cullinane C, Hicks RJ, Pearson RB, Johnstone RW, McArthur GA, Phillips WA. 2012. An activating *Pik3ca* mutation couples with Pten loss is sufficient to initiate ovarian tumorigenesis in mice. J Clin Invest 122:553–557.

Kurek KC, Luks VL, Ayturk UM, Alomari AI, Fishman SJ, Spencer SA, Mulliken JB, Bowen ME, Yamamoto GL, Kozakewich HP, Warman ML. 2012. Somatic mosaic activating mutations in *PIK3CA* cause CLOVES syndrome. Am J Hum Genet 90:1108–1115.

Lee JH, Huynh M, Silhavy JL, Kim S, Dixon-Salazar T, Heiberg A, Scott E, Bafna V, Hill KJ, Collazo A, Funari V, Russ C, Gabriel SB, Mathern GW, Gleeson JG. 2012. De novo somatic mutations in components of the PI3K-AKT3-mTOR pathway cause hemimegalencephaly. Nat Genet 44:941–945.

Lee JW, Soung YH, Kim SY, Lee HW, Park WS, Nam SW, Kim SH, Lee JY, Yoo NJ, Lee SH. 2005. PIK3CA gene is frequently mutated in breast carcinomas and hepatocellular carcinomas. Oncogene 24: 1477–1480.

Levine DA, Bogomolniy F, Yee CJ, Lash A, Barakat RR, Borgen PI, Boyd J. 2005. Frequent mutation of PIK3CA gene in ovarian and breast cancers. Clin Cancer Res 11:2875–2878.

Li VS, Wong CW, Chan TL, Chan AS, Zhao W, Chu KM, So S, Chen X, Yuen ST, Leung SY. 2005. Mutations of *PIK3CA* in gastric adenocarcinomas. BMC Cancer 5:29.

Lindhurst MJ, Sapp JC, Teer JK, Johnston JJ, Finn EM, Peters K, Turner J, Cannons JL, Bick D, Blakemore L, Blumhorst C, Brockmann K, Calder P, Cherman N, Deardorff MA, Everman DB, Golas G, Greenstein RM, Kato BM, Keppler-Noreuil KM, Kuznetsov SA, Miyamoto RT, Newman K, Ng D, O'Brien K, Rothenberg S, Schwartzentruber DJ, Singhal V, Tirabosco R, Upton J, Wientroub S, Zackai EH, Hoag K, Whitewood-Neal T, Robey PG, Schwartzberg PL, Darling TN, Tosi LL, Mullikin JC, Biesecker LG. 2011. A mosaic activating mutation in AKT1 associated with the Proteus syndrome. New Engl J Med 365:611–619.

Lindhurst MJ, Parker VER, Payne F, Sapp JC, Rudge S, Harris J, Witdowski AM, Zhang Q, Groeneveld MP, Scott CE, Daly A, Huson SM, Tosi LL, Cunningham ML, Darling TN, Geer J, Gucev Z, Sutton VR, Tziotzios C, Dixon AK, Halliwell T, O'Rahilly SO, Savage DB, Wakelam MJO, Barroso I, Biesecker LG, Semple RK. 2012. Mosaic overgrowth with fibroadipose hyperplasia is caused by somatic activating mutations in *PIK3CA*. Nat Genet 44:928–933.

Lindhurst MJ, Wang J, Bloomhardt HM, Witkowski AM, Singh LN, Bick DP, Gambello MJ, Powell CM, Lee CCR, Darling TN, Biesecker LG. 2014. *AKT1 gene* mutation levels are correlated with the type of dermatologic lesions in patients with Proteus syndrome. J Invest Dermatol 134:543–546.

Lo Re AE, Fernancdex-Barrena MG, Almada LL, Mils LD, Elsawa SF, Lund G, Ropolo A, Molejon MI, Vaccaro MI, Fernandex-Zapico ME. 2012. Novel AKT1-GLI3-VMP1 pathway mediates KRAS oncogene-induced autophagy in cancer cells. J Biol Chem 287:25325–25334.

Lu P, Minowada G, Martin GR. 2005. Increasing *Fgf4* expression in the mouse limb bud causes polysyndactyly and rescues the skeletal defects that results from loos of *Fgf8* function. Development 133:33–42.

Marsh DJ, Trahair TN, Martin JL, Chee WY, Walker J, Kirk EP, Baxter RC, Marshall GM. 2008. Rapamycin treatment for a child with germline PTEN mutation. Nat Clin Pract Oncol 5:357–361.

Meyer DS, Brinkhaus H, Muller M, Cardiff RD, Bentires-Alj M. 2011. Luminal expression of *PIK3CA* mutant H1047R in the mammary gland induces heterogeneous tumors. Cancer Res 71:4344–4351.

Mirzaa GM, Conway RL, Gripp KW, Lerman-Sagie T, Siegel DH, deVries LS, Lev D, Kramer N, Hopkins E, Graham JM, Jr. Dobyns WB. 2012. Megalencephaly-capillary malformation (MCAP) and megalencephaly-polydactyly-polymicrogyria-hydrocephalus (MPPH) syndromes: Two closely related disorders of brain overgrowth and abnormal brain and body morphogenesis. Am J Med Genet A 158A:269–291.

Mirzaa GM, Rivière JB, Dobyns WB. 2013a. Megalencephaly syndromes and activating mutations in the PI3K-AKT pathway: MPPH and MCAP. Am J Med Genet C Semin Med Genet 163:122–130.

Mirzaa GM, Conway R, Graham JM, Dobyns WB. 2013b. *PIK3CA*-related segmental overgrowth. GeneReviews Pagon RA, Adam MP, Bird TD, et al. editors. Seattle (WA): University of Washington, Seattle. 1993–2014.

Ogina S, Liao X, Chan AT. 2013. Aspirin, *PIK3CA* mutation, and colorectal-cancer survival. N Engl J Med 368:289–290.

Poduri A, Evrony GD, Cai X, Elhosary PC, Beroukhim R, Lehtinen MK, Hills LB, Heinzen EL, Hill A, Hill RS, Barry BJ, Bourgeois BF, Riviello JJ, Barkovich AJ, Black PM, Ligon KL, Walsh CA. 2012. Somatic activation of AKT3 causes hemispheric developmental brain malformations. Neuron 74:41–48.

Printz C. 2013. Aspirin extends life of some patients with colorectal cancer. Cancer 119:472–473.

Raffan E, Semple RK. 2011. Next generation sequencing—Implications for clinical practice. Br Med Bull 99:53–71.

Rios JJ, Paria N, Burns DK, Israel BA, Cornelia R, Wise CA, Ezaki M. 2013. Somatic gain-of-function mutations in *PIK3CA* in patients with macrodactyly. Hum Mol Genet 22:444–451.

Rivière JB, Mirzaa GM, O'Roak BJ, Beddaoui M, Alcantara D, Conway RL, St-Onge J, Schwartzentruber JA, Gripp KW, Nikkel SM, Worthylake T, Sullivan CT, Ward TR, Butler HE, Kramer NA, Albrecht B, Armour CM, Armstrong L, Caluseriu O, Cytrynbaum C, Drolet BA, Innes AM, Lauzon JL, Lin AE, Mancini GM, Meschino WS, Reggin JD, Saggar AK, Lerman-Sagie T, Uyanik G, Weksberg R, Zirn B, Beaulieu CL. Finding of Rare Disease Genes (FORGE) Canada Consortium. Majewski J, Bulman DE, O'Driscoll M, Shendure J, Graham JM, Jr. Boycott KM, Dobyns WB, 2012. De novo germline and postzygotic mutations in *AKT3*, *PIK3R2* and *PIK3CA* cause a spectrum of related megalencephaly syndromes. Nat Genet 44:934–940.

Sahin IH, Garrett C. 2013. Aspirin, PIK3CA mutation and colorectal-cancer survival. N Engl J Med 368:289.

Samuels Y, Wang Z, Bardelli A, Silliman N, Ptak J, Szabo S, Yan H, Gazdar A, Powell SM, Riggins GJ, Willson JK, Markowitz S, Kinzler KW, Vogelstein B, Velculescu VE. 2004. High frequency of mutations of the *PIK3CA* gene in human cancers. Science 304:554.

Sapp JC, Turner JT, van de Kamp JM, van Kijk FS, Lowry RB, Biesecker LG. 2007. Newly delineated syndrome of congenital lipomatous overgrowth, vascular malformations, and epidermal nevi (CLOVE syndrome) in seven patients. Am J Med Genet A 143A:2944–2958.

Shirley MD, Tang H, Gallione CJ, Baugher JD, Frelin LP, Cohen B, North PE, Marchuk DA, Comi AM, Pevsner J. 2013. Sturge-Weber syndrome and port-wine stains caused by somatic mutation in GNAQ. N Engl J Med 368:1971–1979.

Tosi LL, Sapp JC, Allen ES, O'Keefe RJ, Biesecker LG. 2011. Assessment and management of the orthopedic and other complications of Proteus syndrome. J Child Orthop 5:319–327.

Tziotzios C, Walters M, Biesecker LG. 2011. More than just a big thumb. QJM 104:989–991.

Velho S, Oliveira C, Ferreira A, Ferreira AC, Suriano G, Schwartz S, Jr. Duval A, Carneiro F, Machado JC, Hamelin R, Seruca R. 2005. The prevalence of *PIK3CA* mutation in gastric and colon cancers. Eur J Cancer 41:1649–1654.

Viudez A, Hernandez I, Vera R. 2013. Aspirin, *PIK3CA* mutation, and colorectal-cancer survival. N Engl J Med 368:289.

Vivanco I, Sawyers CL. 2002. The phosphatidylinositol 2-Kinase AKT pathway in human cancer. Nat Rev Cancer 2:489–501.

Whiteman EL, Cho H, Birnbaum MJ. 2002. Role of Akt/protein kinase B in metabolism. Trends Endocrinol Metab 13:444–451.

Yuan TL, Cantley LC. 2008. PI3K pathway alterations in cancer: Variations on a theme. Oncogene 27:5497–5510.

SUPPORTING INFORMATION

Additional Supporting Information may be found in the online version of this article at the publisher's web-site.